Modulation vector of the Fulde-Ferrell-Larkin-Ovchinnikov state in CeCoIn₅ revealed by high-resolution magnetostriction measurements

Shunichiro Kittaka, Yohei Kono, Kaito Tsunashima, and Daisuke Kimoto
Department of Physics, Chuo University, Bunkyo-ku, Tokyo 112-8551, Japan

Makoto Yokoyama ⬤
Faculty of Science, Ibaraki University, Mito, Ibaraki 310-8512, Japan
and Institute of Quantum Beam Science, Ibaraki University, Mito, Ibaraki 310-8512, Japan

Yusei Shimizu ⬤
Institute for Materials Research (IMR), Tohoku University, Oarai, Ibaraki 311-1313, Japan

Toshiro Sakakibara and Minoru Yamashita ⬤
Institute for Solid State Physics, University of Tokyo, Kashiwa, Chiba 277-8581, Japan

Kazushige Machida
Department of Physics, Ritsumeikan University, Kusatsu, Shiga 525-8577, Japan

The Fulde-Ferrell-Larkin-Ovchinnikov (FFLO) state is an exotic superconducting phase formed by Cooper pairs with finite center-of-mass momentum q. On theoretical grounds, the superconducting order parameter in the FFLO state is spatially modulated along the q vector, and the emergence of an associated anisotropy is expected at the phase transition from the Abrikosov state to the FFLO state. Here, we report the results of high-resolution magnetostriction measurements for a single crystal of CeCoIn₅ around $B \parallel c$. We find two anomalies in the magnetostriction along the c axis, parallel to the magnetic-field orientation. In sharp contrast, this B_K anomaly disappears in the magnetostriction along the a-axis direction, perpendicular to the magnetic-field orientation. To explain this uniaxial expansion, we suggest a possibility that the FFLO transition occurs slightly below the upper critical field, and the FFLO modulation vector parallel to the applied magnetic field gives rise to the anisotropic response.

The Fulde-Ferrell-Larkin-Ovchinnikov (FFLO) state [1,2] is a prototype example of the so-called pair density wave superconductivity (inset of Fig. 1) [3,4] where translational symmetry is spontaneously broken in addition to $U(1)$ gauge symmetry. It is a topologically interesting object [5] and has been long sought in a wide range of research fields, from condensed matter [6] to cold neutral atoms [7–9]. In order to realize the FFLO state, several strict conditions are required to be fulfilled [6]. For example, the system must be very clean because the FFLO state is easy to be broken by a small amount of impurities and/or defects. Furthermore, the orbital pair-breaking effect needs to be sufficiently weaker than the Pauli-paramagnetic effect. Therefore, for a long period of time, there were few experimental reports on the FFLO state. However, in recent years, there has been a gradual increase in the number of materials that are expected to realize the FFLO state, such as quasi-low-dimensional organic superconductors [10–18], iron-based superconductors [19–21], and Sr₂RuO₄ [22,23].

The heavy-fermion superconductor CeCoIn₅ is also a good candidate realizing the FFLO state. It has been well established as a spin-singlet $d_{x^2-y^2}$-wave superconductor [24–29].

In the heavy-fermion system, the orbital pair-breaking effect is sufficiently weak due to the large effective mass of heavy quasiparticles. Indeed, the emergence of a first-order superconducting transition at the upper critical field B_{c2} below 0.7 K, as well as the suppression of B_{c2} at low temperatures, have been reported in CeCoIn₅ [30–32], indicating that the Pauli-paramagnetic effect overcomes the orbital pair-breaking effect. Moreover, a specific-heat anomaly has been found inside the superconducting phase under an in-plane magnetic field [33,34]. This anomaly may be attributed to a transition from the uniform superconducting state, i.e., Abrikosov vortex state, to the FFLO state [35,36]. The double-peak spectral structure detected slightly below B_{c2} from nuclear magnetic resonance (NMR) experiments also supports the presence of a high-field phase [37–40]. Thus, CeCoIn₅ has a high-field superconducting phase, particularly for $B \parallel ab$.

However, it remains controversial whether this high-field phase is the FFLO phase. From NMR and neutron-scattering experiments, it has been revealed that, in the high-field phase for $B \parallel ab$ (the so-called Q phase), a spin density wave (SDW) order coexists with superconductivity [41,42]. Because the magnetic structure in this Q phase is independent of the
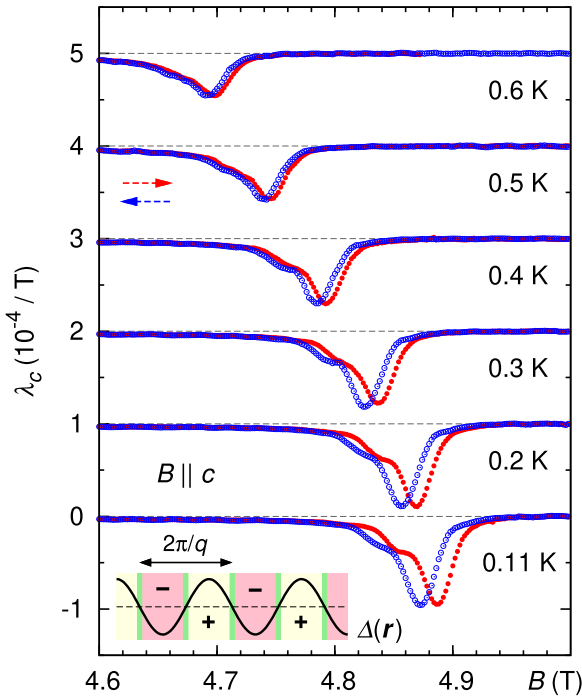
FIG. 1. The c-axis magnetostriction coefficient $\lambda_c(B) = (\partial L_c/\partial B)/L_c$ at several temperatures for $B \parallel c$. Each set of data is shifted vertically by 10^{-4} T^{-1} for clarity. Closed (open) circles represent the data taken in the field-increasing (-decreasing) processes. Inset shows a schematic image of the spatial modulation of the order parameter $\Delta(r)$ in the FFLO state along the modulation vector q.

direction of the in-plane magnetic field, it was suggested that the Q phase is not driven by the FFLO state [43]. Recent theoretical studies and thermal conductivity measurements have also suggested that the FFLO state competes with the SDW phase [44]. The coexistence of SDW order and superconductivity complicates the interpretation of the high-field phase in CeCoIn$_5$ for $B \parallel ab$.

Then, it seems reasonable to turn our attention to a possible high-field phase in CeCoIn$_5$ for $B \parallel c$ because the magnetic ordering is quickly suppressed by tilting the magnetic field from the ab plane [45]. Indeed, no spectrum broadening is reported in the recent NMR measurements for $B \parallel c$ [46], showing the absence of the magnetic instability around B_{c2}. Therefore, if the high-field phase exists in $B \parallel c$, it is expected to be a pure FFLO phase. From NMR experiments, double-peak structure, similar to the one for $B \parallel ab$ [37,40], has been observed in the range 4.7 T $\lesssim B \lesssim B_{c2}$ for $B \parallel c$ [38,39]. However, there is no other crucial evidence for the occurrence of the high-field phase in $B \parallel c$. In order to provide further experimental evidence for the FFLO transition in $B \parallel c$, we have performed high-resolution magnetostriction measurements.

High-quality single crystals of CeCoIn$_5$ were grown by the self-flux method. This paper focuses on the results of one of three samples used; the others are shown in Secs. I and II of the Supplemental Material (SM) [47]. The isothermal magnetostriction, $\Delta L_i(B) = L_i(B) - L_i(B_0)$, and thermal expansion, $\Delta L_i(T) = L_i(T) - L_i(T_0)$, along the i ($i = a$ or c) axis were measured using a homemade capacitance dilatometer in a

dilution refrigerator (Kelvinox AST Minisorb, Oxford). Here, B_0 (T_0) represents a selected constant field (temperature). The sample lengths were 1.34 and 0.9 mm along the a and c axes, respectively. The crystalline axes were determined using an x-ray back-scattering Laue camera (RASCO-BL II, Rigaku). A magnetic field B was generated using a 7-T split-pair magnet in the horizontal x direction. For L_c (L_a) measurements, the measurement direction of the compact dilatometer was set to be parallel to the x (z) axis, so that the magnetic field can be applied along the c axis. The field-angle ϕ dependences of L_c and L_a were investigated by rotating the sample together with the refrigerator around the vertical z direction using a stepper motor at the top of the magnet Dewar, where ϕ denotes the field angle measured from the c axis to the b axis. Although, due to the nonrectangular shape of the sample, the a axis was not perfectly aligned to the measurement direction of L_a, this misalignment does not affect the conclusion of this paper (see Sec. IV of SM [47] for more details).

Figure 1 presents the field derivative data, $\lambda_c(B) = (\partial L_c/\partial B)/L_c$ at several temperatures in the field-increasing and -decreasing processes. As shown in Fig. 1, $|\lambda_c(B)|$ shows a sharp peak at B_{c2} with a hysteresis that develops below 0.6 K, demonstrating the first-order superconducting transition at B_{c2} [30,31]. The sharp peak of $|\lambda_c(B)|$ at B_{c2} demonstrates the high quality of the present sample. Most remarkably, slightly below B_{c2}, a kink anomaly appears at B_K concomitantly with the development of the hysteresis at low temperatures. We confirm the reproducibility of this B_K anomaly in the measurement of another sample (see Sec. II of SM [47]). Indeed, the specific-heat anomaly close to B_{c2} is suggested in the previous report [33]. It should be noted that our high-resolution magnetostriction measurements performed at small steps of $\sim$0.002 T near B_{c2} allow us to clearly detect the B_K anomaly in $B \parallel c$ that was not reported in the previous work [48,49].

The inset of Fig. 2 displays the linear thermal expansion coefficient α_c in zero field, where α_c denotes $(\partial L_c/\partial T)/L_c$. A sharp anomaly is seen in α_c at $T_c = 2.25$ K in zero field; α_c exhibits no sign of T_c distribution within the resolution limit. Figure 2 shows the thermal expansion $\Delta L_c(T)/L_c$ at several magnetic fields for $B \parallel c$. The hysteresis behavior in $\Delta L_c(T)$ becomes prominent above 4.8 T in the superconducting state, while no difference was found between cooling and warming in the $\Delta L_c(T)$ data at 4.7 T. The B_K anomaly is less clearly detected from the thermal expansion (temperature scan) because the superconducting transition at T_c affects the thermal expansion in wide temperature range (see Sec. III of SM [47]).

Figure 3(a) shows the field-temperature phase diagram of CeCoIn$_5$ for $B \parallel c$, in which the positions of B_{c2} and B_K are determined by the two peaks in $d\lambda_c/dB$ as indicated by arrows in Fig. 3(b). The B_K anomaly becomes indistinguishable above 0.6 K due to the broadening of the B_{c2} transition. The tricritical point between the FFLO, homogeneous Abrikosov vortex, and paramagnetic normal states can be determined by the onset critical field above which the superconducting transition becomes first order. To determine this critical magnetic field, we estimate the temperature dependence of the magnetic hysteresis at B_{c2} between the field-increasing and -decreasing measurements (Fig. 3). The magnetic hysteresis between these measurements appears at around 0.6 K and 4.7 T for $B \parallel c$,
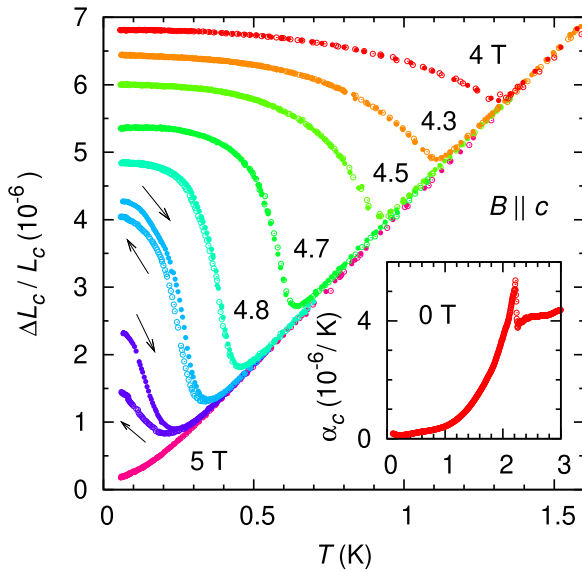
FIG. 2. Thermal expansion $\Delta L_c/L_c$ measured at 5, 4.89, 4.85, 4.8, 4.7, 4.5, 4.3, and 4 T (from bottom to top) for $B \parallel c$. Closed and open circles represent the data taken in the warming and cooling processes, respectively. Inset shows temperature dependence of the thermal expansion coefficient $\alpha_c = (\partial L_c/\partial T)/L_c$ along the c axis at 0 T.

which is suggested as the tricritical point (see also Fig. S4 of SM [47]).

Due to the anisotropy in B_{c2} of CeCoIn$_5$ ($B_{c2}^{\parallel ab}/B_{c2}^{\parallel c} \sim 2.4$), the superconducting transition can be induced by rotating a magnetic field from the c axis when $B_{c2}^{\parallel c} < B < B_{c2}^{\parallel ab}$. Figure 4(a) shows the field-angle ϕ dependence of $\Delta L_c(\phi) = L_c(\phi) - L_c(\phi_0)$ measured at 0.11 K under a magnetic field of 5 T rotated within the bc plane. Here, ϕ_0 is a selected constant field angle. A first-order superconducting transition with clear hysteresis has been observed in $\Delta L_c(\phi)$ at $\phi \sim 14°$. The field-angle derivative data, $\lambda_{\phi,c}(\phi) = (\partial L_c/\partial \phi)/L_c$, are presented in Fig. 4(b). In $\lambda_{\phi,c}(\phi)$, the B_K anomaly can be seen at $\phi \sim 16°$, which is compatible with the one observed in $\lambda_c(B)$ (Fig. 1). The height of the B_K anomaly does not depend on the direction of the field angle sweep, whereas the B_{c2} anomaly at $\phi \sim 14°$ is more prominent for the transition from normal to superconducting state [closed symbols in Fig. 4(b)] than for the transition from superconducting to normal state [open symbols in Fig. 4(b)]. Thus, two anomalies exhibit qualitatively different features, likely stemming from different origins.

Furthermore, the a-axis magnetostriction $\Delta L_a(\phi) = L_a(\phi) - L_a(\phi_0)$ of the same sample was measured under a rotating magnetic field within the plane normal to the measurement direction, i.e., the approximate bc plane. Figures 4(a) and 4(b) show the ϕ dependences of $\Delta L_a(\phi)$ and its angle derivative $\lambda_{\phi,a}(\phi) = (\partial L_a/\partial \phi)/L_a$, respectively. The change in $\Delta L_a/L_a$ at B_{c2} is 2×10^{-6}, about half of the change in $\Delta L_c/L_c$. These results are consistent with the previous report [48,49]. In sharp contrast to $\lambda_{\phi,c}(\phi)$, $\lambda_{\phi,a}(\phi)$ shows one sharp transition without the second anomaly at B_K. The observed peak in $|\lambda_{\phi,a}(\phi)|$ has similar features to the main peak in $|\lambda_{\phi,c}|$ (see Sec. IV of SM [47]).
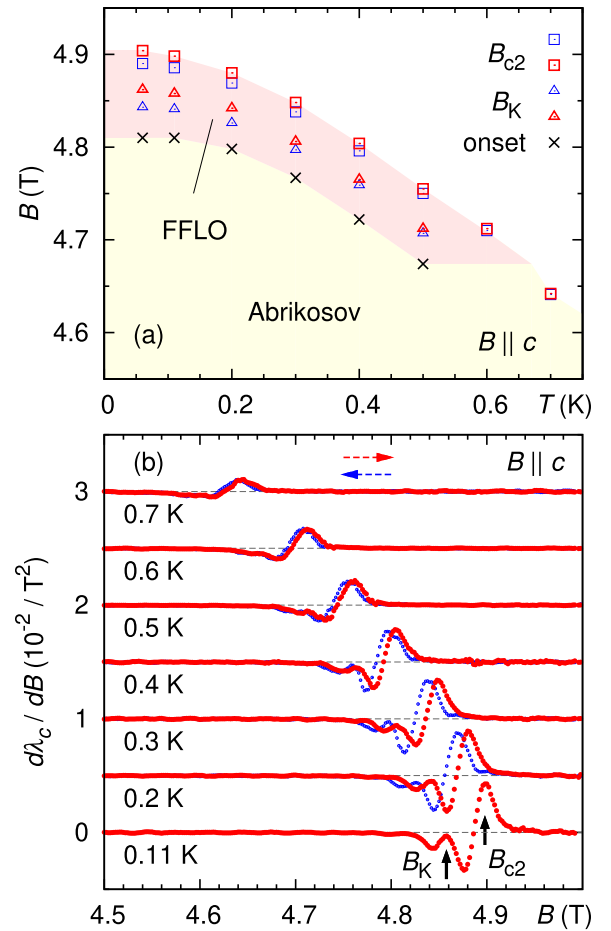

FIG. 3. (a) Field-temperature phase diagram of CeCoIn$_5$ for $B \parallel c$. (b) Field dependence of $d\lambda_c/dB$ at several temperatures. Both increasing and decreasing field data are shown above 0.2 K (only the former at 0.11 K). Each set of data in (b) is shifted vertically by 5×10^{-3} T^{-2} for clarity. The positions of B_{c2} [squares in (a)] and B_K (triangles) are determined by large and small peaks in $d\lambda_c/dB$, respectively, as indicated by solid arrows in (b). The symbols shown in red (blue) are determined from the field-increasing (-decreasing) data. Crosses represent the field above which $\lambda_c(B)$ starts to change markedly toward B_K with increasing B, possibly corresponding to a boundary between the Abrikosov state and the FFLO state.

As shown in the inset of Fig. 4(b), both $\lambda_{\phi,c}$ and $\lambda_{\phi,a}$ are symmetric with respect to the angle direction. This symmetric angle dependence in $\lambda_{\phi,c}$ eliminates the possibility that the B_K anomaly is caused by a domain with a tilted c axis in the sample, because such a domain should show the B_K anomaly at a smaller or larger field angle when the magnetic field is rotated in the other direction. The results of the Gaussian fits to $\lambda_{\phi,c}$ [a solid line in Fig. 4(b)] reveal that a full width at half-maximum (FWHM) of the B_K anomaly ($\sim 1.42° \pm 0.05°$) [a dash-dotted line in Fig. 4(b)] is narrower than the FWHM of the B_{c2} anomaly ($\sim 1.65° \pm 0.02$) [a dashed line in Fig. 4(b)] (see Sec. IV of SM [47] for more details). From this fact, the B_K anomaly is unlikely to be caused by sample inhomogeneities that exist in regions not detected from the L_a measurements because suppression of B_{c2} by impurities and/or defects usually results in a wider distribution of B_{c2}.
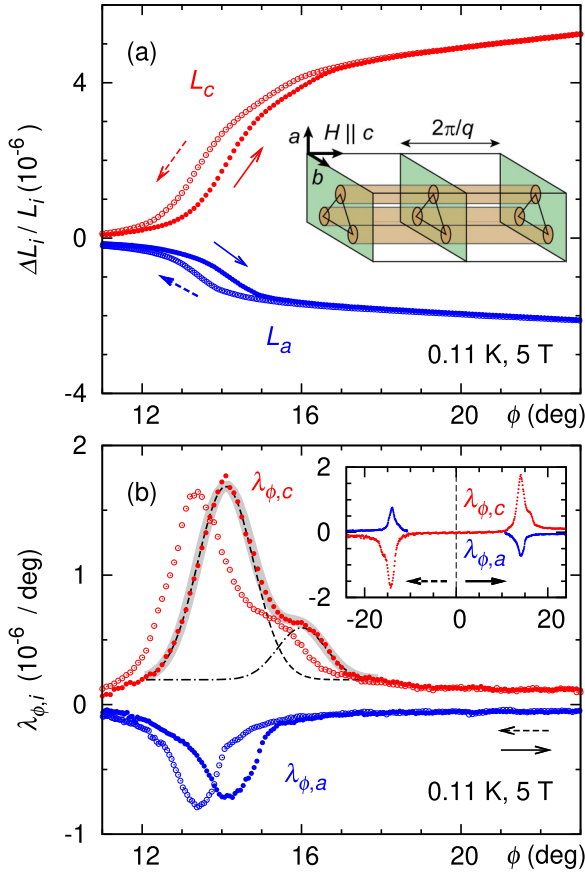
FIG. 4. Field angle ϕ dependence of (a) $\Delta L_i / L_i$ at 0.11 K and 5 T, and (b) their field-angle derivatives, $\lambda_{\phi,i} = (\partial L_i / \partial \phi)/L_i$ ($i = a$ or c). Closed (open) symbols represent the data taken in the ϕ-increasing (decreasing) process. The gray solid line in (b) represents the simulation spectrum consisting of two Gaussian functions (dashed and dash-dotted lines). Inset in (a) shows a schematic view of the flux lines and the FFLO modulation. The periodic nodal planes, separated by $L = 2\pi/q$, run perpendicular to the flux lines that form a vortex lattice in the ab plane. Inset in (b) shows a wider view of $\lambda_{\phi,i}(\phi)$ in the ϕ-increasing (-decreasing) process for $\phi > 0$ ($\phi < 0$).
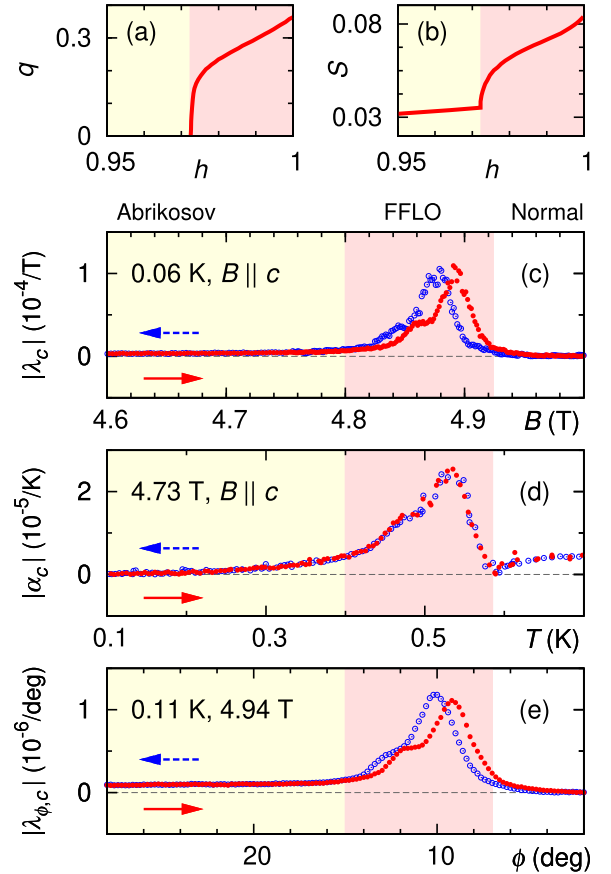

FIG. 5. (a) The wave number q normalized by the coherent length and (b) the normalized entropy $S = S_s(T)/S_n(T_c)$ as a function of $h = H/H_{c2}$, taken from Ref. [36]. Here, S_s (S_n) is the entropy in the superconducting (normal) state. (c) $|\lambda_c|$ as a function of B at $T = 0.06$ K for $B \parallel c$. (d) $|\alpha_c|$ as a function of T at $B = 4.73$ T for $B \parallel c$. (e) $|\lambda_{\phi,c}|$ as a function of the angle ϕ at $B = 4.94$ T and $T = 0.11$ K. The yellow and the pink colored regions represent the Abrikosov state and the FFLO state, respectively; the boundary in $|\lambda_c|$ and $|\lambda_{\phi,c}|$ ($|\alpha_c|$) is determined by the onset of the B_K anomaly [inferred from the phase diagram in Fig. 3(a)].

Let us discuss why the B_K anomaly exists only in L_c when $B \parallel c$. The most plausible origin is the formation of the FFLO state with $\mathbf{q} \parallel \mathbf{B}$, as detailed below.

The FFLO state is characterized by a periodic spatial modulation of the superconducting order parameter $\Delta(\mathbf{r})$ with the wave vector $\mathbf{q}$. The direction of the $\mathbf{q}$ vector is determined by the combination of the relative stabilities between the vortex lattice configuration and the nesting condition, where the Zeeman-split Fermi surfaces are maximally touched under the translation by $\mathbf{q}$. When the FFLO state is realized in a superconductor with an isotropic spherical Fermi surface, the $\mathbf{q}$ vector directs parallel to the field direction; $\mathbf{q} \parallel \mathbf{B}$. This is because the vortex lattice configuration is least perturbed by the formation of the FFLO state, otherwise the two factors of the relative stabilities, i.e., vortex lattice configuration and nesting condition, interfere each other [see the inset of Fig. 4(a)]. For CeCoIn$_5$, it is necessary to consider the nesting condition based on the actual band structure [50–52]. The main Fermi surfaces of CeCoIn$_5$ are the two heavy electron bands (α and

β bands) with the warped cylindrical shape, open along the c axis at the four corners of the tetragonal Brillouin zone. For $B \parallel c$, the optimal $\mathbf{q}$ direction is parallel to the c axis under this uniaxial symmetry situation because the two Fermi surfaces are nested circularly around the warped neck region, as confirmed by a model calculation [53].

In the FFLO state, $\Delta(\mathbf{r})$ has the nodal planes perpendicular to the $\mathbf{q}$ direction whose separation is given by $L = 2\pi/q$, where $q = |\mathbf{q}|$. Thus, the flux lines intersect perpendicular to the nodal planes, as shown in the inset of Fig. 4(a). The nodal plane accommodates the excess imbalanced spin component produced by the applied magnetic field through the Pauli paramagnetic effect because the sign change of $\Delta(\mathbf{r})$ allows the Andreev bound state at the zero energy position [54]. The nodal plane or domain wall contains the excess paramagnetic moment, accompanying the longitudinal strain wave [35,36].

Upon entering the FFLO state from the Abrikosov vortex state with increasing B, the wave number q quickly increases from $q = 0$ at the transition field as shown in Fig. 5(a). This

abrupt increase is a universal feature, independent of theoretical frameworks [55]. This rapid growth of q results in an upward field dependence common to other physical quantities such as the entropy [Fig. 5(b)], the density of state, and the paramagnetic moment. Therefore, L_c is expected to show a similar dependence on B, T and ϕ near the FFLO transition. Indeed, field, temperature, and field-angle derivatives of the change in $\Delta L_c/L_c$, corresponding to λ_c, the linear thermal expansion coefficient α_c, and $\lambda_{\phi,c}$ respectively, exhibit quick change at the Abrikosov-FFLO boundary along the three different paths (B, T and ϕ), as shown in Figs. 5(c)–5(e). In this phase transition, the phase boundary between the Abrikosov and FFLO states corresponds to the lower onset field as shown in Fig. 5(b). Therefore, the phase boundary is determined by the lower onset of the B_K anomaly [crosses in Fig. 3(a)], rather than its peak position.

The absence of the B_K anomaly in the L_a measurements is also consistent with the FFLO scenario, because the spatial modulation brought by the FFLO transition runs only along $q \parallel c$ with keeping the uniformity in the ab plane [see the inset of Fig. 4(a)]. Indeed, even if the a-axis length is maximally distorted according to the Poisson's ratio (0.3 for typical metals), the B_K anomaly in $|\lambda_{\phi,a}|$ would be at most 0.15×10^{-6}/deg, which should be less prominent than the one observed in $|\lambda_{\phi,c}|$. This anisotropic magnetostriction response of the B_K anomaly is reminiscent of a FFLO transition suggested in κ-(BEDT-TTF)$_2$Cu(NCS)$_2$ [18], whose acoustic response depends on the sound propagation direction. Moreover, the observed field range ΔB_{LO}, which is estimated by the width of the magnetic field area between the onset of the

B_K anomaly and B_{c2} [the pink region in Fig. 5(c)], relative to B_{c2}, $\Delta B_{LO}/B_{c2} \sim 2.4\%$, is comparable to the theoretical calculation ($\sim 2.7\%$) [36]. Thus, the B_K anomaly can be well understood if the FFLO state with $q \parallel c$ is formed in CeCoIn$_5$ for $B \parallel c$, which should be scrutinized by further measurements in future to directly detect the spatial modulation of the superconducting gap structure.

In summary, we have performed high-resolution magnetostriction measurements on CeCoIn$_5$ along the c and a axes in the magnetic field applied around the c axis. We find a double superconducting transition at B_K and B_{c2} in the c-axis magnetostriction. On the other hand, this B_K anomaly is absent in the a-axis magnetostriction of the same sample. To explain this anisotropic expansion, we suggest a possibility that the anisotropic length changes of L_c and L_a are a direct manifestation of the FFLO formation, and that the modulation vector q points parallel to the field direction along the c axis. The characteristic changes in the $|\lambda_c(B)|$ curves with an upward curvature are consistent with the theoretical prediction assuming the FFLO formation. This study paves the way for determining the q-vector orientation of the FFLO state from the magnetostriction in different measurement directions.

[1] P. Fulde and R. A. Ferrell, Phys. Rev. **135**, A550 (1964).

[2] A. I. Larkin and Y. N. Ovchinnikov, Zh. Eksp. Teor. Fiz. **47**, 1136 (1964).

[3] D. F. Agterberg, J. S. Davis, S. D. Edkins, E. Fradkin, D. J. V. Harlingen, S. A. Kivelson, P. A. Lee, L. Radzihovsky, J. M. Tranquada, and Y. Wang, Annu. Rev. Condens. **11**, 231 (2020).

[4] D. F. Agterberg and H. Tsunetsugu, Nature Phys. **4**, 639 (2008).

[5] T. Mizushima, K. Machida, and M. Ichioka, Phys. Rev. Lett. **95**, 117003 (2005).

[6] Y. Matsuda and H. Shimahara, J. Phys. Soc. Jpn. **76**, 051005 (2007).

[7] M. W. Zwierlein, A. Schirotzek, C. H. Schunck, and W. Ketterle, Science **311**, 492 (2006).

[8] G. B. Partridge, W. Li, R. I. Kamar, Y. Liao, and R. G. Hulet, Science **311**, 503 (2006).

[9] T. Mizushima, K. Machida, and M. Ichioka, Phys. Rev. Lett. **94**, 060404 (2005).

[10] J. Singleton, J. A. Symington, M.-S. Nam, A. Ardavan, M. Kurmoo, and P. Day, J. Phys.: Condens. Matter **12**, L641 (2000).

[11] S. Uji, H. Shinagawa, T. Terashima, T. Yakabe, Y. Terai, M. Tokumoto, A. Kobayashi, H. Tanaka, and H. Kobayashi, Nature (London) **410**, 908 (2001).

[12] S. Uji, T. Terashima, M. Nishimura, Y. Takahide, T. Konoike, K. Enomoto, H. Cui, H. Kobayashi, A. Kobayashi, H. Tanaka, M.

Tokumoto, E. S. Choi, T. Tokumoto, D. Graf, and J. S. Brooks, Phys. Rev. Lett. **97**, 157001 (2006).

[13] J. Shinagawa, Y. Kurosaki, F. Zhang, C. Parker, S. E. Brown, D. Jérome, J. B. Christensen, and K. Bechgaard, Phys. Rev. Lett. **98**, 147002 (2007).

[14] S. Yonezawa, S. Kusaba, Y. Maeno, P. Auban-Senzier, C. Pasquier, K. Bechgaard, and D. Jérome, Phys. Rev. Lett. **100**, 117002 (2008).

[15] S. Yonezawa, S. Kusaba, Y. Maeno, P. Auban-Senzier, C. Pasquier, and D. Jérome, J. Phys. Soc. Jpn. **77**, 054712 (2008).

[16] H. Mayaffre, S. Krämer, M. Horvatić, C. Berthier, K. Miyagawa, K. Kanoda, and V. F. Mitrović, Nature Phys. **10**, 928 (2014).

[17] S. Imajo, T. Kobayashi, A. Kawamoto, K. Kindo, and Y. Nakazawa, Phys. Rev. B **103**, L220501 (2021).

[18] S. Imajo, T. Nomura, Y. Kohama, and K. Kindo, Nature Commun. **13**, 5590 (2022).

[19] P. Burger, F. Hardy, D. Aoki, A. E. Böhmer, R. Eder, R. Heid, T. Wolf, P. Schweiss, R. Fromknecht, M. J. Jackson, C. Paulsen, and C. Meingast, Phys. Rev. B **88**, 014517 (2013).

[20] C.-w. Cho, J. H. Yang, N. F. Q. Yuan, J. Shen, T. Wolf, and R. Lortz, Phys. Rev. Lett. **119**, 217002 (2017).

[21] S. Kasahara, Y. Sato, S. Licciardello, M. Čulo, S. Arsenijević, T. Ottenbros, T. Tominaga, J. Böker, I. Eremin, T. Shibauchi, J. Wosnitza, N. E. Hussey, and Y. Matsuda, Phys. Rev. Lett. **124**, 107001 (2020).

[22] S. Kittaka, S. Nakamura, T. Sakakibara, N. Kikugawa, T. Terashima, S. Uji, D. A. Sokolov, A. P. Mackenzie, K. Irie, Y. Tsutsumi, K. Suzuki, and K. Machida, J. Phys. Soc. Jpn. **87**, 093703 (2018).

[23] K. Kinjo, M. Manago, S. Kitagawa, Z. Q. Mao, S. Yonezawa, Y. Maeno, and K. Ishida, Science **376**, 397 (2022).

[24] N. J. Curro, B. Simovic, P. C. Hammel, P. G. Pagliuso, J. L. Sarrao, J. D. Thompson, and G. B. Martins, Phys. Rev. B **64**, 180514(R) (2001).

[25] Y. Kohori, Y. Yamato, Y. Iwamoto, T. Kohara, E. D. Bauer, M. B. Maple, and J. L. Sarrao, Phys. Rev. B **64**, 134526 (2001).

[26] K. Izawa, H. Yamaguchi, Y. Matsuda, H. Shishido, R. Settai, and Y. Ōnuki, Phys. Rev. Lett. **87**, 057002 (2001).

[27] K. An, T. Sakakibara, R. Settai, Y. Ōnuki, M. Hiragi, M. Ichioka, and K. Machida, Phys. Rev. Lett. **104**, 037002 (2010).

[28] M. P. Allan, F. Massee, D. K. Morr, J. V. Dyke, A. W. Rost, A. P. Mackenzie, C. Petrovic, and J. C. Davis, Nature Phys. **9**, 468 (2013).

[29] B. B. Zhou, S. Misra, E. H. da Silva Neto, P. Aynajian, R. E. Baumbach, J. D. Thompson, E. D. Bauer, and A. Yazdani, Nature Phys. **9**, 474 (2013).

[30] A. Bianchi, R. Movshovich, N. Oeschler, P. Gegenwart, F. Steglich, J. D. Thompson, P. G. Pagliuso, and J. L. Sarrao, Phys. Rev. Lett. **89**, 137002 (2002).

[31] T. Tayama, A. Harita, T. Sakakibara, Y. Haga, H. Shishido, R. Settai, and Y. Onuki, Phys. Rev. B **65**, 180504(R) (2002).

[32] T. P. Murphy, D. Hall, E. C. Palm, S. W. Tozer, C. Petrovic, Z. Fisk, R. G. Goodrich, P. G. Pagliuso, J. L. Sarrao, and J. D. Thompson, Phys. Rev. B **65**, 100514(R) (2002).

[33] A. Bianchi, R. Movshovich, C. Capan, P. G. Pagliuso, and J. L. Sarrao, Phys. Rev. Lett. **91**, 187004 (2003).

[34] H. A. Radovan, N. A. Fortune, T. P. Murphy, S. T. Hannahs, E. C. Palm, S. W. Tozer, and D. Hall, Nature (London) **425**, 51 (2003).

[35] M. Ichioka, H. Adachi, T. Mizushima, and K. Machida, Phys. Rev. B **76**, 014503 (2007).

[36] K. M. Suzuki, K. Machida, Y. Tsutsumi, and M. Ichioka, Phys. Rev. B **101**, 214516 (2020).

[37] K. Kakuyanagi, M. Saitoh, K. Kumagai, S. Takashima, M. Nohara, H. Takagi, and Y. Matsuda, Phys. Rev. Lett. **94**, 047602 (2005).

[38] K. Kumagai, M. Saitoh, T. Oyaizu, Y. Furukawa, S. Takashima, M. Nohara, H. Takagi, and Y. Matsuda, Phys. Rev. Lett. **97**, 227002 (2006).

[39] K. Kumagai, T. Oyaizu, N. Kondoh, H. Shishido, and Y. Matsuda, J. Phys.: Conf. Ser. **150**, 052135 (2009).

[40] K. Kumagai, H. Shishido, T. Shibauchi, and Y. Matsuda, Phys. Rev. Lett. **106**, 137004 (2011).

[41] B.-L. Young, R. R. Urbano, N. J. Curro, J. D. Thompson, J. L. Sarrao, A. B. Vorontsov, and M. J. Graf, Phys. Rev. Lett. **98**, 036402 (2007).

[42] M. Kenzelmann, T. Strässle, C. Niedermayer, M. Sigrist, B. Padmanabhan, M. Zolliker, A. D. Bianchi, R. Movshovich, E. D. Bauer, J. L. Sarrao, and J. D. Thompson, Science **321**, 1652 (2008).

[43] M. Kenzelmann, S. Gerber, N. Egetenmeyer, J. L. Gavilano, T. Strässle, A. D. Bianchi, E. Ressouche, R. Movshovich, E. D. Bauer, J. L. Sarrao, and J. D. Thompson, Phys. Rev. Lett. **104**, 127001 (2010).

[44] S.-Z. Lin, D. Y. Kim, E. D. Bauer, F. Ronning, J. D. Thompson, and R. Movshovich, Phys. Rev. Lett. **124**, 217001 (2020).

[45] E. Blackburn, P. Das, M. R. Eskildsen, E. M. Forgan, M. Laver, C. Niedermayer, C. Petrovic, and J. S. White, Phys. Rev. Lett. **105**, 187001 (2010).

[46] T. Taniguchi, S. Kitagawa, M. Manago, G. Nakamine, K. Ishida, and H. Shishido, JPS Conf. Proc. **30**, 011107 (2020).

[47] See Supplemental Material at http://link.aps.org/supplemental/10.1103/PhysRevB.107.L220505 for further details of (I) experimental methods, (II) sample dependence of the *c*-axis magnetostriction, (III) additional thermal expansion data, and (IV) field-angle dependence of the change in the sample length.

[48] V. F. Correa, T. P. Murphy, C. Martin, K. M. Purcell, E. C. Palm, G. M. Schmiedeshoff, J. C. Cooley, and S. W. Tozer, Phys. Rev. Lett. **98**, 087001 (2007).

[49] T. Takeuchi, H. Shishido, S. Ikeda, R. Settai, Y. Haga, and Y. Ōnuki, J. Phys.: Condens. Matter **14**, L261 (2002).

[50] H. Shishido, T. Ueda, S. Hashimoto, T. Kubo, R. Settai, H. Harima, and Y. Onuki, J. Phys.: Condens. Matter **15**, L499 (2003).

[51] R. Settai, H. Shishido, S. Ikeda, Y. Murakawa, M. Nakashima, D. Aoki, Y. Haga, H. Harima, and Y. Ōnuki, J. Phys.: Condens. Matter **13**, L627 (2001).

[52] D. Hall, E. C. Palm, T. P. Murphy, S. W. Tozer, Z. Fisk, U. Alver, R. G. Goodrich, J. L. Sarrao, P. G. Pagliuso, and T. Ebihara, Phys. Rev. B **64**, 212508 (2001).

[53] H. Shimahara, J. Phys. Soc. Jpn. **90**, 044706 (2021).

[54] The formation of the Andreev bound state exactly at the intersection points between flux and nodal plane is prohibited topologically because the phase winding felt by quasiparticles is 2π, not π. See Ref. [5] for more details.

[55] K. Machida and H. Nakanishi, Phys. Rev. B **30**, 122 (1984).